Research Paper

Short-term high-fat diet primes excitatory synapses for long-term depression in orexin neurons

Victoria Linehan, Lisa Fang, and Michiru Hirasawa

Division of Biomedical Sciences, Faculty of Medicine, Memorial University, St. John's, NL, Canada, A1B 3V6

Running Title: High-fat diet unmasks LTD in orexin neurons

Key words: Orexin/Hypocretin, Synaptic plasticity, High-fat diet

Corresponding author:
Michiru Hirasawa PhD, DVM
Division of Biomedical Sciences
Faculty of Medicine, Memorial University
300 Prince Philip Drive
St. John's, NL, Canada
A1B 3V6

Tel: +1-709-864-6573
Fax: +1-709-864-6007
Email: michiru@mun.ca

Key Points Summary

- High-fat diet consumption is a major cause of obesity.

- Orexin neurons are known to be activated by high-fat diet and in turn promote further consumption of high-fat diet.

- Our study shows that excitatory synapses to orexin neurons become amenable to long-term depression (LTD) after 1 week of high-fat diet feeding. However, this effect reverses after 4 weeks of high-fat diet.

- This LTD may be a homeostatic response to high-fat diet to curb the activity of orexin neurons and hence caloric consumption. Adaptation seen after prolonged diet intake may contribute to development of obesity.

Abstract

Overconsumption of high-fat diets is one of the strongest contributing factors to the rise of obesity rates. Orexin neurons are known to be activated by palatable high-fat diet and mediate the activation of the mesolimbic reward pathway, resulting in further food intake. While short-term exposure to high-fat diet is known to induce synaptic plasticity within the mesolimbic pathway, it is unknown if such changes occur in orexin neurons. To investigate this, 3-week old male rats were fed a palatable high-fat western diet (WD) or control chow for 1 week and then *in vitro* patch clamp recording was performed. In the WD condition, an activity-dependent long-term depression (LTD) of excitatory synapses was observed in orexin neurons, but not in chow controls. This LTD was presynaptic and depended on postsynaptic metabotropic glutamate receptor 5 (mGluR5) and retrograde endocannabinoid signaling. WD also increased extracellular glutamate levels, suggesting that glutamate spillover and subsequent activation of perisynaptic mGluR5 may occur more readily in the WD condition. In support of this, pharmacological inhibition of glutamate uptake was sufficient to prime chow control synapses to undergo a presynaptic LTD. Interestingly, these WD effects are transient, as extracellular glutamate levels were similar to controls and LTD was no longer observed in orexin neurons after 4 weeks of WD. In summary, excitatory synapses to orexin neurons become amenable to LTD under palatable

high-fat diet, which may represent a homeostatic mechanism to prevent overactivation of these neurons and to curtail high-fat diet consumption.

Abbreviations

ACSF, artificial cerebrospinal fluid; AM251, 1-(2,4-dichlorophenyl)-5-(4-iodophenyl)-4-methyl-N-1-piperidinyl-1H-pyrazole-3-carboxamide; CB1R, type 1 cannabinoid receptor; Ctrl, control; CPPG, (RS)-α-cyclopropyl-4-phosphonophenylglycine; DAP5, D-2-amino-5-phosophonovalerate; DHK, dihydrokainic acid; DHPG, (S)-3,5-dihydroxyphenylglycine; γDGG, γ-D-glutamylglycine; GLAST, glutamate-aspartate transporter; GLT-1, glutamate transporter-1; HFS, high-frequency stimulation; LTD, long-term depression; LTP, long-term potentiation; mGluR, metabotropic glutamate receptor; MPEP, 6-methyl-2-(phenylethynyl)pyridine; PPR, paired pulse ratio; VTA, ventral tegmental area; WD, western diet

Introduction

Excessive consumption of high-fat diets has become increasingly common in many countries around the world, increasing the risks of serious health outcomes such as cardiovascular diseases, metabolic syndrome, and obesity (Cordain *et al.*, 2005). Caloric consumption beyond metabolic need is driven by the rewarding value of high-fat food, which is mediated by the mesolimbic dopamine pathway (Volkow *et al.*, 2011). Activation of this pathway by high-fat diet involves orexin signaling. Specifically, orexin neurons are activated by short-term high-fat diet (Chang *et al.*, 2004; Valdivia *et al.*, 2014) and subsequently stimulate dopamine neurons within the ventral tegmental area (VTA), thereby activating the mesolimbic pathway (Zheng *et al.*, 2007; Valdivia *et al.*, 2014; Baimel *et al.*, 2017). This suggests that a positive feedback loop between high-fat diet, orexin neurons and VTA dopamine neurons drives overconsumption of high-fat diet. However, high-fat diet may suppress the orexin system in the long term, as chronic high-fat diet decreases orexin gene and peptide levels in animals (Novak *et al.*, 2010; Tanno *et al.*, 2013). Thus, the regulation of the orexin system may change over the course of high-fat diet feeding.

While high-fat diet is known to induce various types of functional and structural plasticity within the reward circuitry (Johnson & Kenny, 2010; Vucetic *et al.*, 2012; Sharma *et al.*, 2013; Labouèbe *et al.*, 2013), plastic changes in orexin neurons during high-fat diet are poorly understood. There has been one study that investigated synaptic plasticity in orexin neurons after chronic high-fat diet, which found changes in type 1 cannabinoid receptor (CB1R)-expressing presynaptic terminals apposed to orexin neurons (Cristino *et al.*, 2013). However, to our knowledge there has been no report on the effect of short-term high fat diet on synaptic plasticity of these neurons. Plasticity of excitatory synapses should impact the excitability of orexin neurons, as excitatory synaptic contacts to these neurons significantly outnumber inhibitory ones and influence their basal firing rate (Li *et al.*, 2002; Horvath & Gao, 2005). Moreover, orexin neurons are known to display plasticity of excitatory synapses under various physiological states, such as fasting (Horvath & Gao, 2005) and sleep deprivation (Rao *et al.*, 2007), which has been postulated to affect foraging and arousal, respectively.

In this study, we investigated the effect of short-term exposure to a palatable high-fat western diet (WD) on excitatory transmission to orexin neurons. We identified a novel form of long-term plasticity of these synapses after one week of WD feeding, which was diminished after a prolonged WD exposure. These changes may alter orexin network properties and underlie their physiological role in reward-based feeding during short- and long-term high-fat diet.

Methods

Ethical Approval

All animal procedures were conducted as approved by the Memorial University's Institutional Animal Care Committee under the guidelines of the Canadian Council on Animal Care.

Animals and Diets

Male 3-week old Sprague-Dawley rats were obtained either from Charles River (Quebec, Canada) or Memorial University's Breeding Colony. Upon arrival, rats were singly housed and given either WD (TestDiet AIN-76A: 4.55kcal/g, 40% fat, 16% protein, and 44% carbohydrates by caloric content) or a standard rodent chow (LabDiet 5010: 3.08kcal/g, 12.7% fat, 28.7% protein, and 58.5% carbohydrates). Body weight and food intake were measured weekly. A total of 90 rats were used in this study.

Electrophysiological Recording

After 1 or 4 weeks of feeding, rats were anesthetized with isoflurane inhalation and sacrificed by decapitation. The brain was removed and acute 250-µm hypothalamic slices were generated on a vibratome (VT-1000, Leica Microsystems) in artificial cerebrospinal fluid (ACSF) composed of 126mM NaCl, 2.5mM KCl, 1.2mM NaH$_2$PO$_4$, 1.2mM MgCl$_2$, 18mM NaHCO$_3$, 2.5mM glucose, and 2mM CaCl$_2$. ACSF was chilled on ice for 5-10 minutes before slicing. After dissection, hypothalamic slices were incubated at 32-34℃ for

30-35 minutes in ACSF then left at room temperature until experiments were performed. ACSF was continuously bubbled with 95% O_2/5% CO_2 gas.

Slices were transferred to a recording chamber, perfused with ACSF (1-2mL per minute at 30-32℃) and visualized with infrared-differential interference contrast optics (DM LFSA, Leica Microsystems). Whole-cell patch clamp recordings were performed on neurons within the lateral hypothalamus/perifornical area using Multiclamp 700B and pClamp 9 or 10 software (Molecular Devices, Sunnyvale, CA, US). Signals were filtered at 1kHz and digitized at 5-10kHz. An internal solution containing 123mM K gluconate, 2mM $MgCl_2$, 1mM KCl, 0.2mM EGTA, 10mM HEPES, 5mM Na_2ATP, 0.3mM NaGTP, and 2.7mM biocytin was used to fill glass patch electrodes with a final tip resistance between 3-5MΩ.

Afferent fibers were electrically stimulated via a glass pipette filled with ACSF placed medial to recorded neurons, using a voltage that results in approximately 50% of maximum synaptic response. Evoked EPSCs were pharmacologically isolated using the $GABA_A$ channel blocker picrotoxin (50μM) and recorded every 15 seconds at a holding potential of –70mV. These EPSCs are largely mediated by AMPA receptors but not kainite receptors (Alberto & Hirasawa, 2010). Paired pulses were applied at 10 or 50Hz to assess paired pulse ratio (PPR) defined as the amplitude of EPSC2 divided by that of EPSC1. To induce activity-dependent synaptic plasticity, a high frequency stimulation (HFS) was applied to the afferents using the same stimulation electrode while in current clamp mode, consisting of 100 pulses at 100Hz every 4 seconds, 10 times. Long-term synaptic plasticity was assessed at 25-30 minutes post-HFS or at 25-30 minutes following the start of DHPG application. Series/access resistance was assessed by applying 20mV, 50ms hyperpolarizing pulses every 15 seconds. Cells that showed a change in these parameters by more than 20% were excluded from further analysis.

Identification of Orexin Neurons

A series of 600-ms hyperpolarizing and depolarizing current steps were applied in current clamp mode to identify putative orexin neurons. Orexin neurons display a distinct electrophysiological response to this current protocol compared to other cell types in the

region which allow for high accuracy cell-type identification (Alberto *et al.*, 2011; Linehan *et al.*, 2015). Specifically, orexin neurons display spontaneous firing, uniphasic afterhyperpolarizing potential, H-current, and rebound depolarization following relief from hyperpolarization.

To confirm the neurochemical phenotype, post hoc immunohistochemistry was performed in a subset of cells (116 of 175 cells). During recording, cells were filled with biocytin via the recording pipette and subsequently brain slices were fixed in 10% formalin for at least 24 hours. Slices were then incubated with a goat anti-orexin A IgG (1:2000; SC8070, Santa Cruz Biotechnology, Santa Cruz, CA) for 3 days, followed by Alexa 594-conjugated donkey anti-goat IgG (1:500) and Alexa 350-conjugated streptavidin (1:500). Colocalization of biocytin with orexin A staining was assessed on an epifluorescence microscope. Electrophysiologically-identified orexin neurons were correctly confirmed by immunohistochemistry in 115 of 116 cells tested (99.1% success rate), and the one immuno-negative cell was removed. A total of 174 cells that displayed the characteristic electrophysiological fingerprint of orexin neurons were used in the analysis.

Drugs

Drugs were prepared as stock solutions and were diluted with ACSF to the final concentration immediately prior to experiment except for GDPβS, which was added to the internal solution at its final concentration (2mM) in place of GTP. DAP5, MPEP, AM251, CPPG and DHK were bath applied for 10 minutes before HFS up until 5 minutes post-HFS, unless indicated otherwise. DHPG and γDGG were bath applied for 5 minutes. Picrotoxin, GDPβS, and AM251 (1-(2,4-dichlorophenyl)-5-(4-iodophenyl)-4-methyl-N-1-piperidinyl-1H-pyrazole-3-carboxamide) were from Sigma Aldrich (Oakville, ON, CA); DAP5 and γ-D-glutamylglycine (γDGG) were from Abcam (Cambridge, MA, US); and 6-methyl-2-(phenylethynyl)pyridine (MPEP), dihydrokainic acid (DHK), (RS)-α-cyclopropyl-4-phosphonophenylglycine (CPPG), and (S)-3,5-dihydroxyphenylglycine (DHPG) were from Tocris Bioscience (Minneapolis, MN, US).

Statistical Analysis

The number of samples is reported in the nested model where N/n represents the number of cells/ the number of animals. Data are expressed as the mean ± SEM and p<0.05 was considered significant. Statistical analyses were performed using Prism 6.0 (GraphPad Software Inc.). Unpaired or paired t-test and one-way or two-way ANOVA with post hoc Holm-Sidak test were performed on the data as applicable.

Results

To examine the effects of high-fat diet on orexin neurons, rats were fed with either a WD or a standard chow (Ctrl) for up to 4 weeks. Rats on WD consistently consumed more calories throughout the feeding period compared to chow controls (Fig.1A,C; Ctrl n=20 rats vs WD n=22 rats; weekly caloric intake, two-way ANOVA: $F_{1,40}$=34.16, p<0.0001; total caloric intake, unpaired t-test: t_{40}=5.845, p<0.0001); however, this did not result in any difference in body weight at any time point (Fig.1B; two-way ANOVA: $F_{1,40}$=1.020, p=0.3185). At the end of the 4-week feeding, there was no difference in body weight (Fig. 1D; unpaired t-test: t_{40}=1.488, p=0.1446) or total weight gain between groups (Fig. 1E; unpaired t-test: t_{40}=1.702, p=0.0966). Following the feeding period, patch clamp recordings were performed on orexin neurons at two time points: after 1 week of feeding when these neurons are known to be activated by high-fat diet (Wortley *et al.*, 2003; Valdivia *et al.*, 2014), and at 4 weeks, when orexin gene expression has been shown to first decrease (Novak *et al.*, 2010).

After 1 week of feeding, all orexin neurons tested in the WD condition displayed a long-term depression (LTD), resulting in approximately a 50% reduction on average in EPSC amplitude (Fig.2A-C; n=6/4, baseline vs post-HFS, paired t-test: t_5=2.815, p=0.0373). In contrast, chow control orexin neurons did not display a consistent response. A fraction of cells (2 out of 7 cells) displayed a long-term potentiation (LTP), defined as an increase in EPSC amplitude by more than 20% of baseline values, while others showed no change (Fig.2A-C; n=7/4, baseline vs post-HFS, paired t-test: t_6=1.079, p=0.3218). Collectively, EPSC amplitude post-HFS was significantly different between chow control and WD (Fig.2C; unpaired t-test: t_{11}=3.933, p=0.0023). The LTD in the WD group was

accompanied by an increase in PPR (Fig.2A,D; baseline vs post-HFS, paired t-test: $t_5=6.250$, p=0.0015) but there was no PPR change in chow controls (Fig.2D; baseline vs post-HFS, paired t-test: $t_6=0.1598$, p=0.8783; Ctrl vs WD, unpaired t-test: $t_{11}=2.335$, p=0.0395). Thus, LTD in the WD condition has a presynaptic locus of expression.

Since WD unmasked a robust LTD in orexin neurons, we sought to determine the mechanism underlying this plasticity using brain slices from WD-fed rats. NMDA receptors are commonly involved in long-term synaptic plasticity, however, the NMDA receptor antagonist DAP5 (50µM) failed to significantly influence the HFS-induced changes in EPSC amplitude (Fig.3A,C; HFS n=6/4 vs. HFS+DAP5 n=8/5, one-way ANOVA, $t_{16}=0.9014$, p=0.3807) or PPR (Fig.3D; HFS vs HFS+DAP5, one-way ANOVA, $t_{16}=1.901$, p=0.0755). Another glutamate receptor that could mediate presynaptic LTD is metabotropic glutamate receptor 5 (mGluR5) (Robbe *et al.*, 2002). We found that LTD was attenuated by the mGluR5-specific antagonist, MPEP (20-40µM) (Fig.3B-D; EPSC amplitude: HFS n=6/4 vs HFS+ MPEP n=5/4, one-way ANOVA, $t_{16}=3.447$, p=0.0066; PPR: HFS vs HFS+MPEP, one-way ANOVA, $t_{16}=3.878$, p=0.0027). Further supporting an mGluR5 involvement, the group 1 mGluR agonist DHPG (50µM) induced a presynaptic LTD on its own (Fig.3E,F; n=13/7, paired t-test: EPSC amplitude $t_{12}=9.158$, p<0.0001; PPR $t_{12}=2.771$, p=0.0169) and occluded HFS-induced LTD (Fig.3E,G-I; HFS n=6/4 vs HFS post-DHPG n=6/3, unpaired t-test: EPSC amplitude $t_{10}=4.212$, p=0.0018; PPR $t_{10}=3.855$, p=0.0032). Taken together, these results suggest that LTD unmasked by WD is due to an mGluR5-dependent mechanism.

To test the role of postsynaptic cell in LTD, 2mM GDPβS was added to the pipette solution and allowed to diffuse into the cell for 10 minutes prior to baseline recording. We have shown previously that this concentration of GDPβS and procedure inhibits G protein signaling within orexin neurons (Parsons *et al.*, 2012). We found that GDPβS blocked both the WD-induced reduction in EPSC amplitude (Fig.4A-C; HFS n=6/4 vs HFS+GDPβS n=6/5, unpaired t-test, $t_{10}=2.865$, p=0.0168) and the increase in PPR (Fig.4C; HFS vs HFS+GDPβS, unpaired t-test, $t_{10}=4.271$, p=0.0016). These data indicates that postsynaptic G protein signaling is required, which supports mGluR5 involvement. Since this LTD is presynaptic, this result suggests a retrograde transmitter such as endocannabinoids must be

involved (Robbe *et al.*, 2002). Consistent with this idea, the CB1R antagonist AM251 (5µM) blocked HFS-induced LTD (Fig.4D,F; EPSC amplitude: HFS n=6/4 vs AM251+HFS n=5/4, one-way ANOVA, t_{14}=2.985, p=0.0196; PPR: HFS vs AM251+HFS, one-way ANOVA, t_{14}=2.020, p=0.1220). However, endocannabinoid signaling is only important for the induction of LTD as AM251 had no effect on the maintenance of LTD when applied 20-30 minutes after HFS (Fig.4E,F; EPSC amplitude: HFS n=6/4 vs HFS+AM251 n=6/3, one-way ANOVA, t_{14}=0.5330, p=0.6024; PPR: HFS vs. HFS+AM251, one-way ANOVA, t_{14}=0.6448, p=0.5295). Furthermore, DHPG was unable to induce LTD in the presence of AM251, indicating that CB1R is downstream of mGluR5 (Fig.4G,I; EPSC amplitude: DHPG n=13/7 vs AM251+DHPG n=6/3, one-way ANOVA, t_{23}=2.679, p=0.0266; PPR: DHPG vs AM251+DHPG, one-way ANOVA, t_{23}=3.699, p=0.0024). Similar to the HFS-induced LTD, AM251 applied 15 minutes following DHPG wash did not affect DHPG-LTD (Fig.4H, I; EPSC amplitude: DHPG vs DHPG+AM251 n=7/4, one-way ANOVA, t_{23}=1.478, p=0.1531; PPR: DHPG vs DHPG+AM251, one-way ANOVA, t_{23}=0.1855, p=0.8544). These results indicate that LTD in orexin neurons is dependent on postsynaptic mGluR5 and retrograde endocannabinoid signaling.

It remains unknown why LTD is consistently observed in orexin neurons in the WD condition but not in chow-fed controls. One possibility is that orexin neurons do not express functional mGluR5 receptors in chow conditions. However, pharmacologically activating group 1 mGluRs in chow controls using the group 1-specific mGluR agonist DHPG also led to a presynaptic LTD (Fig.5A-D; ESPC amplitude, n=7/5: baseline vs post-DHPG, paired t-test: t_6=4.421, p=0.0045; PPR: baseline vs post-DHPG, paired t-test: t_6=2.973, p=0.0249). Thus, the molecular machinery necessary for mGluR5-dependent LTD is intact even in chow-fed condition.

Interestingly, the magnitude of DHPG-induced LTD was smaller in WD (Fig.5B,C; Ctrl n=7/5 vs WD n=13/7, unpaired t-test: t_{18}=2.217, p=0.0397), which may be an indication that endogenously established LTD was occluding the effect of DHPG. If so, presynaptic glutamate release would be inhibited, which should be observed as an increase in PPR. This indeed appeared to be the case since the baseline PPR was higher in the WD group compared to chow controls (Fig.6A,B; Ctrl n=21/14 vs WD n=17/10, unpaired t-test:

$t_{35}=2.615$, p=0.0131). An alternative explanation for this higher PPR is a tonic activation of presynaptic inhibitory group III mGluRs (Acuna-Goycolea *et al.*, 2004); however, the group III mGluR antagonist CPPG (200µM) had no effect on EPSCs in the WD condition (Fig.6C; ESPC amplitude, n=6/3: baseline vs CPPG, paired t-test: $t_5=0.6686$, p=0.5333; PPR: baseline vs CPPG, paired t-test: $t_5=0.7826$, p=0.4693). These results suggest that LTD may have occurred endogenously in orexin neurons in the WD condition and partially occluded the effects of DHPG.

Since the signaling components for group 1 mGluR-dependent LTD are present in both chow and WD conditions, unmasking of HFS-LTD by WD may involve a process upstream of mGluR5 activation, such as synaptic glutamate clearance. To detect any difference in the level of extracellular glutamate during synaptic activity, we used the low affinity, competitive AMPA receptor antagonist γDGG, which competes with endogenous glutamate for AMPA receptors. We determined that 1mM γDGG reduced EPSC amplitude by about 50% at these synapses in chow controls (Liu *et al.*, 1999) (Fig.7A,B; n=7/3: baseline vs γDGG, paired t-test: $t_6=4.771$, p=0.0031) and used this concentration to test the diet effect. In the WD group, it induced significantly less inhibition of EPSCs (Fig.7A,B; n=7/4: baseline vs γDGG, paired t-test: $t_6=5.449$, p=0.0016; Ctrl vs WD, unpaired t-test: $t_{12}=3.443$, p=0.0049). These results indicate that WD induces an increase in extracellular glutamate. However, there was no difference in the decay of EPSCs between WD and chow controls (Fig.7C,D; EPSC decay: Ctrl n=13/8 vs WD n=10/6, unpaired t-test: $t_{21}=0.04987$, p=0.9607), suggesting that the time course of the glutamate transient at the synapse is not affected.

An increase in synaptic glutamate may lead to more glutamate spillover during HFS to activate perisynaptic mGluR5 receptors and their downstream LTD signaling cascade. To test this idea, we used DHK, an inhibitor of the astrocytic glutamate transporter-1 (GLT-1), to inhibit glutamate uptake and facilitate spillover in chow controls. A submaximal concentration of DHK (10-15µM) was used to avoid excitotoxicity, which did not affect EPSC amplitude (n=8/4, baseline: 302.2 ± 70.1pA, DHK: 276.9 ± 73.3pA, paired t-test: $t_7=1.264$, p=0.2466) or decay (Fig.7E; paired t-test: $t_7=0.5208$, p=0.6186). However, in the presence of DHK, chow control synapses expressed a presynaptic LTD in response to HFS

(Fig. 7F-H; DHK+HFS n=6/3, baseline vs post-HFS: EPSC amplitude, paired t-test: $t_5=2.928$, p=0.0327; PPR, paired t-test: $t_5=2.641$, p=0.0459) unlike untreated controls (Ctrl EPSC amplitude: untreated n=7/4 vs DHK n=6/3, two-way ANOVA, $t_{21}=3.843$, p=0.0019; Ctrl PPR: untreated vs DHK, two-way ANOVA, $t_{21}=2.539$, p=0.0378). In contrast, in the WD condition DHK had no additive effect on the magnitude of LTD (Fig.7G,H; WD EPSC amplitude: untreated n=6/4 vs DHK n=6/3, two-way ANOVA, $t_{21}=0.5127$, p=0.6135; WD PPR: untreated vs DHK, two-way ANOVA, $t_{21}=1.952$, p=0.0644). Thus, WD occludes DHK's priming effect, further supporting a role for increased extracellular glutamate in LTD induction.

Finally, we asked whether these WD-induced synaptic changes are long lasting. After 4 weeks of feeding, we found that there was no longer any difference between WD and age-matched chow control groups in extracellular glutamate as measured by the degree of EPSC inhibition by γDGG (Fig.8A,B; 4wCtrl n=8/7 vs 4wWD n=7/6, unpaired t-test: $t_{13}=0.4027$, p=0.6937). Accordingly, neither group expressed HFS-induced LTD (Fig.8C-E; 4wCtrl n=7/3 vs 4wWD n=7/4, EPSC amplitude: unpaired t-test: $t_{12}=0.4771$, p=0.6418, PPR: unpaired t-test: $t_{12}=0.3425$, p=0.7379). Therefore, adaptation to WD occurs at excitatory synapses to orexin neurons.

Discussion

The present study demonstrates that one week of WD feeding primes excitatory synapses to orexin neurons to undergo activity-dependent LTD. WD increases the level of synaptic glutamate, which results in activation of postsynaptic mGluR5 during intense synaptic activity. This leads to endocannabinoid-mediated presynaptic LTD (Fig.9). This priming effect is transient and disappears with longer periods of WD feeding. To our knowledge, this is the first study to describe LTD of excitatory inputs to orexin neurons. Orexin neurons have been shown to synthesize and release endocannabinoids in response to membrane depolarization (Cristino *et al.*, 2013), which in turn acutely inhibit excitatory and inhibitory transmission (Huang *et al.*, 2007; Cristino *et al.*, 2013). Our results show that mGluR5 can also trigger endocannabinoid release from orexin neurons that retrogradely

induces an LTD of excitatory synapses. On the other hand, a previous study described a postsynaptic LTP at these synapses via a cAMP-dependent mechanism (Rao *et al.*, 2007). In our chow controls, HFS induced LTP without a change in PPR in 28.6% of cells tested, which may be explained by the mechanism described above.

While the source of excitatory afferents to orexin neurons tested in this study were not defined, these neurons are known to receive inputs from diverse brain regions involved in energy balance, reward, and sleep/wake control (González *et al.*, 2016). In addition, orexin neurons have wide-ranging projections to brain regions involved in these functions (Peyron *et al.*, 1998). Since LTD was observed in all WD orexin neurons tested, it may not be a mechanism restricted to certain afferent or efferent pathways, but rather it may be a general property that could influence synaptic integration and functional output of these neurons, including arousal, energy balance, motivation, locomotor activity, and sympathetic outflow (Tsujino & Sakurai, 2013).

Although WD feeding was necessary for HFS to induce LTD, pharmacological activation of group 1 mGluRs could induce LTD in both Ctrl and WD conditions. Therefore, the machinery for the mGluR5-CB1R LTD is present and functional under both conditions. Nevertheless, the magnitude of DHPG-induced LTD was smaller in WD compared to chow controls, which may be a partial occlusion by endogenous LTD in WD-fed rats. This is supported by a higher baseline PPR in WD cells suggesting an underlying presynaptic inhibition. Alternatively, a change in cell surface expression (Knackstedt & Schwendt, 2016) or perisynaptic localization of mGluR5 receptors (Sergé *et al.*, 2002) may account for this difference. In addition, chronic high-fat diet has been shown to decrease the number of CB1R-expressing excitatory synapses to orexin neurons (Cristino *et al.*, 2013), which could influence this CB1R-dependent LTD. However, whether this type of synaptic remodeling would occur after 1 week of WD feeding is unknown.

Our study suggests that a change in extracellular glutamate levels underlies the WD-induced unmasking of LTD in orexin neurons. Extracellular glutamate concentration can be influenced by the amount of release, uptake, and diffusion. It is unlikely that WD increases glutamate release, as our results showing an increase in baseline PPR indicate reduced

release. Altered glutamate diffusion can result from a change in synaptic morphology (Piet *et al.*, 2004), which may accompany synaptic remodeling known to be induced by dietary factors in orexin neurons (Horvath & Gao, 2005; Cristino *et al.*, 2013). Extracellular glutamate could also increase if glutamate uptake through transporter activity is decreased. Indeed, hormones influenced by high-fat diet, such as leptin and ghrelin, modulate the expression of astrocytic glutamate transporters GLT-1 and GLAST in the hypothalamus (Fuente-Martín *et al.*, 2012, 2016). Furthermore, we showed that a GLT-1 inhibitor DHK mimics WD and permits HFS-induced LTD in chow control orexin neurons. Thus, a decrease in glutamate transport may be at least partially responsible for increased extracellular glutamate by WD.

The effects of high-fat diet on the orexin system are known to be time-dependent: short exposures to high-fat diet stimulate, while longer exposures suppress the orexin system. For example, after 2 hours of high-fat diet, orexin neurons increase cFos expression (Valdivia *et al.*, 2014) while cell density and mRNA expression increases within 3 weeks of high-fat diet (Wortley *et al.*, 2003, but see Ziotopoulou *et al.*, 2000). Since orexin is necessary for high-fat diet-induced activation of the VTA (Zheng *et al.*, 2007; Valdivia *et al.*, 2014), plasticity at the level of orexin neurons could have functional consequences within the reward circuitry. Moreover, high-fat diet also induces an endocannabinoid-dependent LTD in the VTA and decreases the salience of high-fat diet (Labouèbe *et al.*, 2013). Therefore, LTD at both sites could act in concert to regulate behavioral responses to high-fat diet.

In contrast to these short-term excitatory effects, prolonged exposures (1 to 4 months) reduce orexin gene and peptide levels (Novak *et al.*, 2010; Tanno *et al.*, 2013). In keeping with this, the present study found that LTD was no longer induced after 4 weeks of WD. This adaptation to long-term WD is unlikely to be secondary to weight gain, since in the present study there was no detectable difference in body weight gain of the rats between diet groups for up to 4 weeks of feeding. On the other hand, the animals on WD consistently consumed more calories in fat, therefore the observed synaptic changes may be secondary to an extended presence of triglycerides or dynamic changes in diet-sensitive hormone levels that have time-dependent effects on the brain and behavior (Fuente-Martín

et al., 2012, 2016; Cansell *et al.*, 2014). Alternatively, it may be due to the age of animals, since the developing brain is more vulnerable than adults to the effects of high-fat diet (Morin *et al.*, 2017). Furthermore, the expression of astrocytic glutamate transporters rapidly increases postnatally and continues to increase into adulthood (Furuta *et al.*, 1997). The hypothalamic energy balance circuitry also continues to develop postnatally (Bouret *et al.*, 2004) including orexin neurons (Ogawa *et al.*, 2017). Therefore, it is possible that in young animals, such as those used in this study (3 weeks of age at the start of feeding paradigm), orexin neurons are particularly sensitive to diet-induced plasticity.

In summary, the present study demonstrates a novel mechanism by which WD induces time-dependent metaplasticity in orexin neurons. In a recent paper using a similar WD and animal model as our study, adolescent male Sprague-Dawley rats were shown to display reward hypofunction after 10 days of WD that was normalized by continued WD feeding into adulthood (Rabasa *et al.*, 2016). It is tempting to speculate that priming of orexin neurons to LTD and its reversibility shown in our study contributes to these behavioral response and adaptation to WD. Furthermore, in addition to food intake this synaptic plasticity may also underlie alterations in other physiological functions associated with high-fat diet and obesity, such as diminished wakefulness/alertness and energy expenditure that can be explained by inhibition of orexin neurons (Jenkins *et al.*, 2006; Tanno *et al.*, 2013).

References

Acuna-Goycolea C, Li Y & Van Den Pol AN (2004). Group III metabotropic glutamate receptors maintain tonic inhibition of excitatory synaptic input to hypocretin/orexin neurons. *J Neurosci* **24,** 3013–3022.

Alberto CO & Hirasawa M (2010). AMPA receptor-mediated miniature EPSCs have heterogeneous time courses in orexin neurons. *Biochem Biophys Res Commun* **400,** 707–712.

Alberto CO, Trask RB & Hirasawa M (2011). Dopamine acts as a partial agonist for α2A adrenoceptor in melanin-concentrating hormone neurons. *J Neurosci* **31,** 10671–10676.

Baimel C, Lau BK, Qiao M & Borgland SL (2017). Projection-Target-Defined Effects of Orexin and Dynorphin on VTA Dopamine Neurons. *Cell Rep* **18,** 1346–1355.

Bouret SG, Draper SJ & Simerly RB (2004). Formation of projection pathways from the arcuate nucleus of the hypothalamus to hypothalamic regions implicated in the neural control of feeding behavior in mice. *J Neurosci* **24,** 2797–2805.

Cansell C, Castel J, Denis RGP, Rouch C, Delbes A-S, Martinez S, Mestivier D, Finan B, Maldonado-Aviles JG, Rijnsburger M, Tschöp MH, DiLeone RJ, Eckel RH, la Fleur SE, Magnan C, Hnasko TS & Luquet S (2014). Dietary triglycerides act on mesolimbic structures to regulate the rewarding and motivational aspects of feeding. *Mol Psychiatry* **19,** 1095–1105.

Carlin J, Hill-Smith TE, Lucki I & Reyes TM (2013). Reversal of dopamine system dysfunction in response to high-fat diet. *Obesity (Silver Spring)* **21,** 2513–2521.

Chang G-Q, Karatayev O, Davydova Z & Leibowitz SF (2004). Circulating triglycerides impact on orexigenic peptides and neuronal activity in hypothalamus. *Endocrinology* **145,** 3904–3912.

Cordain L, Eaton SB, Sebastian A, Mann N, Lindeberg S, Watkins B a, O'Keefe JH &

Brand-Miller J (2005). Origins and evolution of the Western diet: health implications for the 21st century. *Am J Clin Nutr* **81,** 341–354.

Cristino L, Busetto G, Imperatore R, Ferrandino I, Palomba L, Silvestri C, Petrosino S, Orlando P, Bentivoglio M, Mackie K & Di Marzo V (2013). Obesity-driven synaptic remodeling affects endocannabinoid control of orexinergic neurons. *Proc Natl Acad Sci U S A* **110,** E2229-38.

Fuente-Martín E, García-Cáceres C, Argente-Arizón P, Díaz F, Granado M, Freire-Regatillo A, Castro-González D, Ceballos ML, Frago LM, Dickson SL, Argente J & Chowen JA (2016). Ghrelin Regulates Glucose and Glutamate Transporters in Hypothalamic Astrocytes. *Sci Rep* **6,** 23673.

Fuente-Martín E, García-Cáceres C, Granado M, de Ceballos ML, Sánchez-Garrido MÁ, Sarman B, Liu Z, Dietrich MO, Tena-Sempere M, Argente-Arizón P, Díaz F, Argente J, Horvath TL & Chowen JA (2012). Leptin regulates glutamate and glucose transporters in hypothalamic astrocytes. *J Clin Invest* **122,** 3900–3913.

Furuta A, Rothstein JD & Martin LJ (1997). Glutamate transporter protein subtypes are expressed differentially during rat CNS development. *J Neurosci* **17,** 8363–8375.

González JA, Jensen LT, Iordanidou P, Strom M, Fugger L & Burdakov D (2016). Inhibitory Interplay between Orexin Neurons and Eating. *Curr Biol* **26,** 2486–2491.

Horvath TL & Gao X-B (2005). Input organization and plasticity of hypocretin neurons: possible clues to obesity's association with insomnia. *Cell Metab* **1,** 279–286.

Huang H, Acuna-Goycolea C, Li Y, Cheng HM, Obrietan K & van den Pol AN (2007). Cannabinoids excite hypothalamic melanin-concentrating hormone but inhibit hypocretin/orexin neurons: implications for cannabinoid actions on food intake and cognitive arousal. *J Neurosci* **27,** 4870–4881.

Jenkins JB, Omori T, Guan Z, Vgontzas AN, Bixler EO & Fang J (2006). Sleep is increased in mice with obesity induced by high-fat food. *Physiol Behav* **87,** 255–262.

Johnson PM & Kenny PJ (2010). Dopamine D2 receptors in addiction-like reward dysfunction and compulsive eating in obese rats. *Nat Neurosci* **13,** 635–641.

Knackstedt LA & Schwendt M (2016). mGlu5 Receptors and Relapse to Cocaine-Seeking: The Role of Receptor Trafficking in Postrelapse Extinction Learning Deficits. *Neural Plast* **2016,** 9312508.

Labouèbe G, Liu S, Dias C, Zou H, Wong JCY, Karunakaran S, Clee SM, Phillips AG, Boutrel B & Borgland SL (2013). Insulin induces long-term depression of ventral tegmental area dopamine neurons via endocannabinoids. *Nat Neurosci* **16,** 300–308.

Li Y, Gao XB, Sakurai T & van den Pol AN (2002). Hypocretin/Orexin excites hypocretin neurons via a local glutamate neuron-A potential mechanism for orchestrating the hypothalamic arousal system. *Neuron* **36,** 1169–1181.

Linehan V, Trask RB, Briggs C, Rowe TM & Hirasawa M (2015). Concentration-dependent activation of dopamine receptors differentially modulates GABA release onto orexin neurons. *Eur J Neurosci* **42,** 1976–1983.

Liu G, Choi S & Tsien RW (1999). Variability of neurotransmitter concentration and nonsaturation of postsynaptic AMPA receptors at synapses in hippocampal cultures and slices. *Neuron* **22,** 395–409.

Morin J, Rodríguez-Durán LF, Guzmán-Ramos K, Perez-Cruz C, Ferreira G, Diaz-Cintra S & Pacheco-López G (2017). Palatable Hyper-Caloric Foods Impact on Neuronal Plasticity. *Front Behav Neurosci* **11,** 19.

Novak CM, Escande C, Burghardt PR, Zhang M, Barbosa MT, Chini EN, Britton SL, Koch LG, Akil H & Levine JA (2010). Spontaneous activity, economy of activity, and resistance to diet-induced obesity in rats bred for high intrinsic aerobic capacity. *Horm Behav* **58,** 355–367.

Ogawa Y, Kanda T, Vogt K & Yanagisawa M (2017). Anatomical and electrophysiological development of the hypothalamic orexin neurons from embryos to neonates. *J Comp Neurol*; DOI: 10.1002/cne.24261.

Parsons MP, Burt J, Cranford A, Alberto C, Zipperlen K & Hirasawa M (2012). Nociceptin induces hypophagia in the perifornical and lateral hypothalamic area. *PLoS One* **7,** e45350.

Peyron C, Tighe DK, van den Pol a N, de Lecea L, Heller HC, Sutcliffe JG & Kilduff TS (1998). Neurons containing hypocretin (orexin) project to multiple neuronal systems. *J Neurosci* **18,** 9996–10015.

Piet R, Vargová L, Syková E, Poulain DA & Oliet SHR (2004). Physiological contribution of the astrocytic environment of neurons to intersynaptic crosstalk. *Proc Natl Acad Sci U S A* **101,** 2151–2155.

Rabasa C, Winsa-Jörnulf J, Vogel H, Babaei CS, Askevik K & Dickson SL (2016). Behavioral consequences of exposure to a high fat diet during the post-weaning period in rats. *Horm Behav* **85,** 56–66.

Rao Y, Liu Z, Borok E, Rabenstein RL, Shanabrough M, Lu M, Picciotto MR, Horvath TL & Gao X (2007). Prolonged wakefulness induces experience-dependent synaptic plasticity in mouse hypocretin/orexin neurons. *J Clin Invest* **117,** 4022–4033.

Robbe D, Kopf M, Remaury A, Bockaert J & Manzoni OJ (2002). Endogenous cannabinoids mediate long-term synaptic depression in the nucleus accumbens. *Proc Natl Acad Sci U S A* **99,** 8384–8388.

Sergé A, Fourgeaud L, Hémar A & Choquet D (2002). Receptor activation and homer differentially control the lateral mobility of metabotropic glutamate receptor 5 in the neuronal membrane. *J Neurosci* **22,** 3910–3920.

Sharma S, Fernandes MF & Fulton S (2013). Adaptations in brain reward circuitry underlie palatable food cravings and anxiety induced by high-fat diet withdrawal. *Int J Obes (Lond)* **37,** 1183–1191.

Tanno S, Terao A, Okamatsu-Ogura Y & Kimura K (2013). Hypothalamic prepro-orexin mRNA level is inversely correlated to the non-rapid eye movement sleep level in high-fat diet-induced obese mice. *Obes Res Clin Pract* **7,** e251-7.

Tsujino N & Sakurai T (2013). Role of orexin in modulating arousal, feeding, and motivation. *Front Behav Neurosci* **7,** 28.

Valdivia S, Patrone A, Reynaldo M & Perello M (2014). Acute high fat diet consumption activates the mesolimbic circuit and requires orexin signaling in a mouse model. *PLoS One* **9,** e87478.

Volkow ND, Wang G-J & Baler RD (2011). Reward, dopamine and the control of food intake: implications for obesity. *Trends Cogn Sci* **15,** 37–46.

Vucetic Z, Carlin JL, Totoki K & Reyes TM (2012). Epigenetic dysregulation of the dopamine system in diet-induced obesity. *J Neurochem* **120,** 891–898.

Wortley KE, Chang G-Q, Davydova Z & Leibowitz SF (2003). Peptides that regulate food intake: orexin gene expression is increased during states of hypertriglyceridemia. *Am J Physiol Regul Integr Comp Physiol* **284,** R1454-65.

Zheng H, Patterson LM & Berthoud H (2007). Orexin signaling in the ventral tegmental area is required for high-fat appetite induced by opioid stimulation of the nucleus accumbens. *J Neurosci* **27,** 11075–11082.

Ziotopoulou M, Mantzoros CS, Hileman SM & Flier JS (2000). Differential expression of hypothalamic neuropeptides in the early phase of diet-induced obesity in mice. *Am J Physiol Endocrinol Metab* **279,** E838-45.

Additional Information

Competing Interests

None

Author Contributions

VL and MH contributed to conception and design of work, and all authors contributed to data acquisition/analysis and writing of the manuscript. All authors approve the final version of the manuscript and agree to be accountable for all aspects of the work.
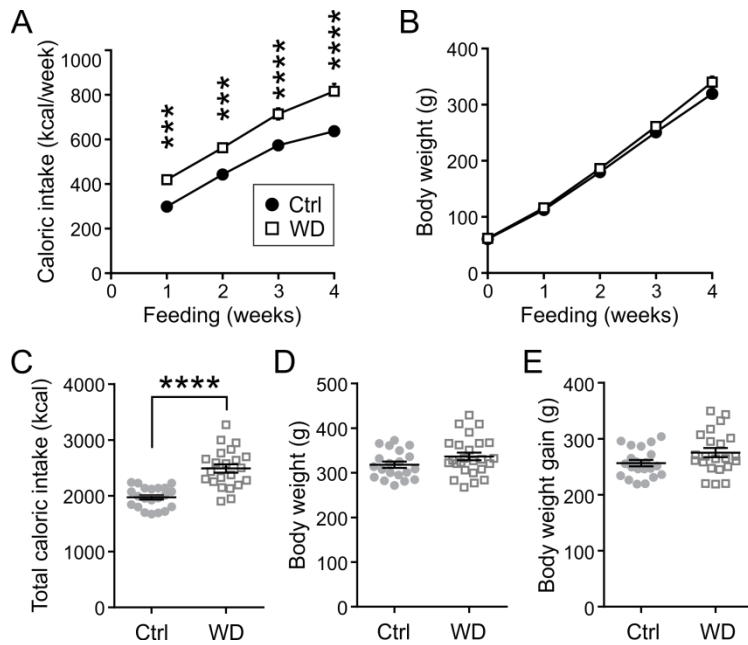
Figure 1: Caloric intake and body weight of rats during WD feeding.
    A) Weekly caloric intake of rats fed with control chow (Ctrl) or WD.
    B) Body weight of rats during the 4-week feeding period.
    C) Total caloric intake during the 4-week feeding period.
    D) Body weight of rats after 4-week feeding (7-week old).
    E) Total body weight gain during the 4-week feeding period.
    ***$p < 0.0005$, ****$p < 0.0001$
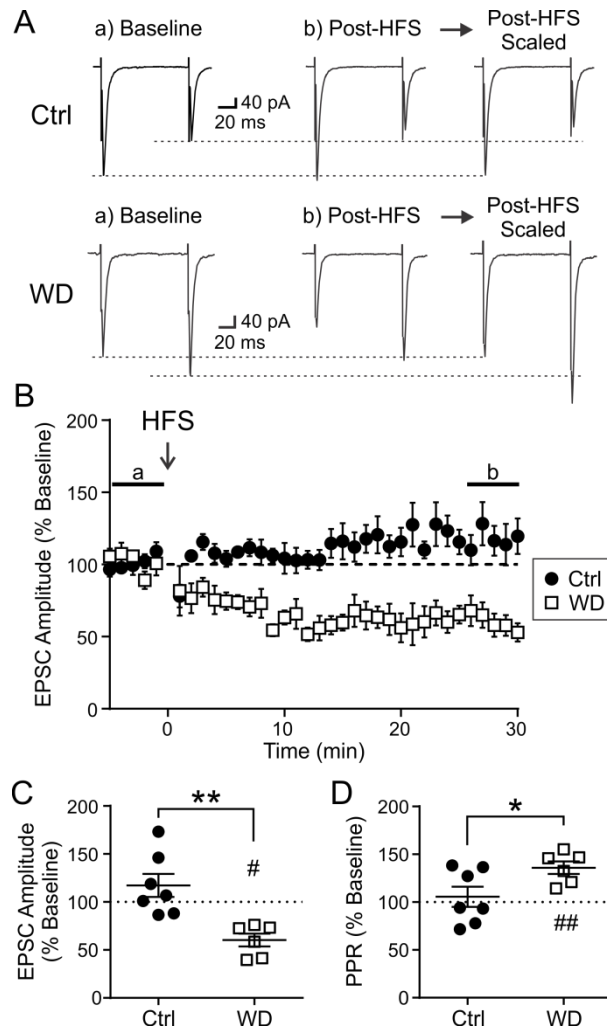
Figure 2: One-week WD primes orexin neurons for HFS-induced presynaptic LTD.
   A) Sample traces showing paired EPSCs of orexin neurons in Ctrl and WD groups at baseline (a) and post-HFS (b), recorded at time points indicated in panel B. Post-HFS traces are scaled so that the first EPSC of baseline and post-HFS are comparable. Dotted reference lines show that the paired pulse ratio (PPR) changed in WD but not in Ctrl.
   B) EPSC amplitude normalized to respective baseline in WD and Ctrl orexin neurons. HFS was applied at time 0.
   C) EPSC amplitude post-HFS (b in panel B) normalized to a 5-minute baseline (a in panel B). For C and D, each symbol denotes an individual orexin neuron.
   D) PPR post-HFS as a percent of baseline in the Ctrl and WD groups.
   *p<0.05, **p<0.005 Ctrl vs WD; #p<0.05, ##p<0.005 baseline vs post-HFS
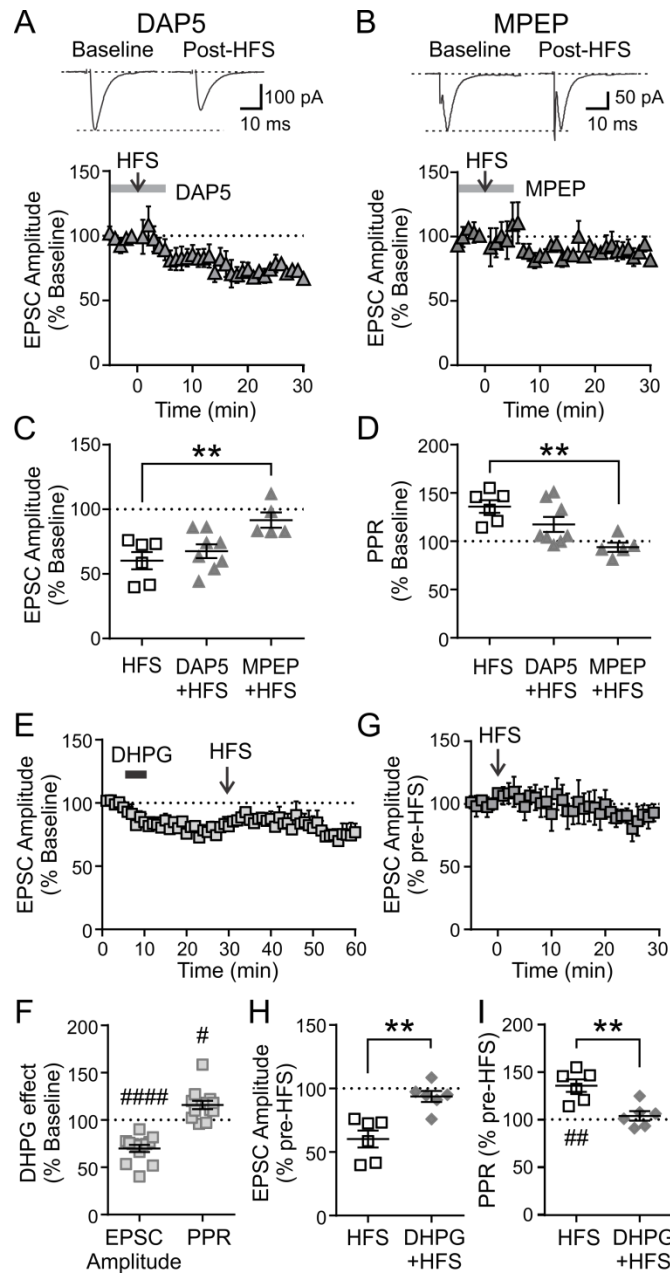
Figure 3: LTD unmasked by WD is mGluR5-dependent.

    A) Top: Sample EPSCs (top) and time-effect plot of EPSC amplitude (bottom) from a WD orexin neuron showing the effect of HFS in the presence of DAP5 (50μM).

    B) Sample EPSCs (top) and time-effect plot of EPSC amplitude (bottom) pre- and post-HFS in the presence of group 1 mGluR antagonist MPEP (20-40μM).

C and D) Summary of EPSC amplitude (C) and PPR (D) post-HFS normalized to baseline. HFS-induced LTD is not affected by DAP5 but blocked by MPEP.

    E) Representative time effect plot of DHPG (50μM) application and subsequent HFS on EPSC amplitude in a WD orexin neuron.

    F) EPSC amplitude and PPR post- DHPG application.

G) EPSC amplitude from the experiment shown in E, normalized to pre-HFS values. Following DHPG application, HFS has no effect on EPSC amplitude.

H and I) Summary of EPSC amplitude (H) and PPR (I) post-HFS normalized to respective baseline without or with prior DHPG application. DHPG occludes HFD-induced LTD in WD orexin neurons.

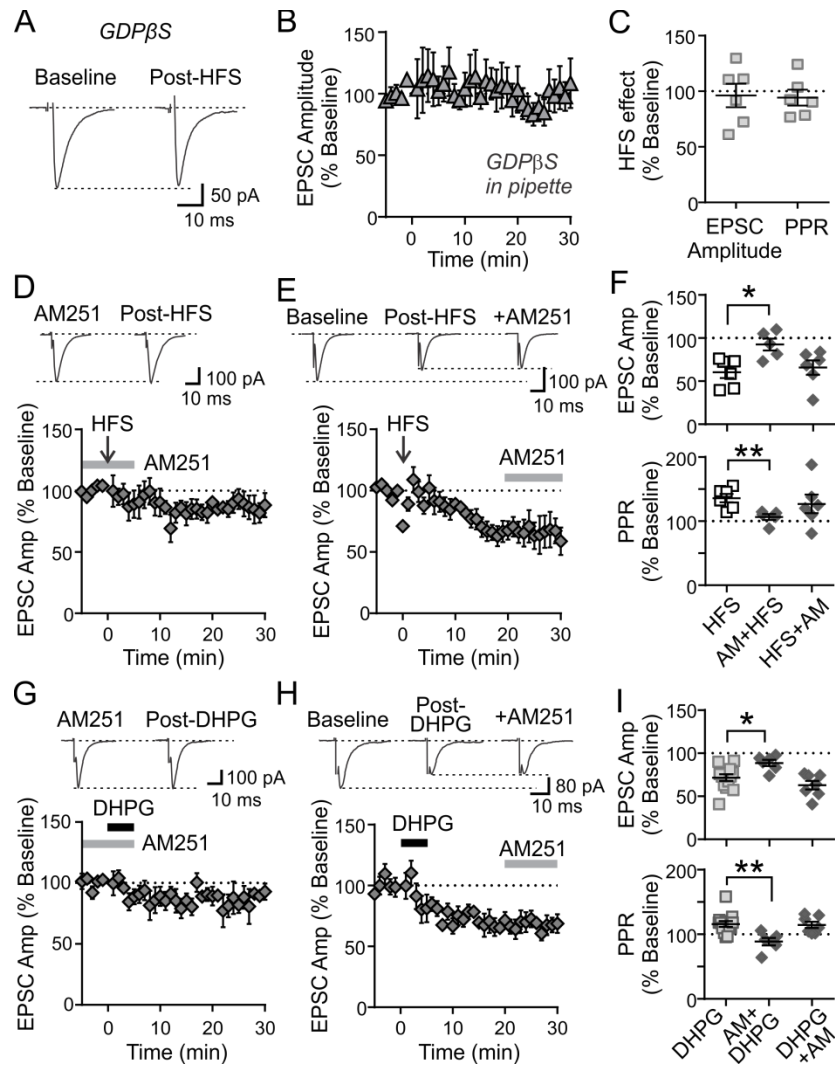**p<0.01 for comparisons of different experimental groups; #p<0.05, ##p<0.005, ####p<0.0001 baseline vs post-treatment

Figure 4: LTD is mediated by retrograde endocannabinoid signaling in orexin neurons.

A) Sample EPSCs recorded from a WD orexin neuron with an inhibitor of G-protein signaling GDPβS (2mM) in the recording pipette.

B) Time-effect plot of EPSC amplitude recorded with GDPβS in the recording pipette.

C) Summary of experiments shown in B. HFS has no effect on EPSC amplitude or PPR when applied in the presence of GDPβS.

D) Sample ESPCs from a WD orexin neuron (top) and time-effect plot of EPSC amplitude (bottom) recorded before and after HFS, applied in the presence of the CB1R antagonist AM251 (AM; 5μM).

E) Sample recording from a WD orexin neuron (top) and time-effect plot of EPSC amplitude (bottom) showing that HFS–induced LTD is not affected by AM251 applied 20-30 minutes after HFS.

F) Summary of experiments shown in D and E. Normalized EPSC amplitude (top) and PPR (bottom) at 25-30 minutes post-HFS in orexin neurons. AM251 prevents LTD

when present during HFS (AM+HFS), but not when applied after LTD is established (HFS+AM).

G) Sample ESPCs from a WD orexin neuron (top) and time-effect plot of EPSC amplitude (bottom) showing lack of effect of DHPG when applied in the presence of AM251.

H) Sample ESPCs from a WD orexin neuron (top) and time-effect plot of EPSC amplitude (bottom) showing that AM251 has no effect on DHPG-induced LTD.

I) Summary of experiments shown in G and H, showing normalized EPSC amplitude (top) and PPR (bottom) post-DHPG. AM251 prevents DHPG-induced LTD when applied concurrently with DHPG (AM+DHPG), but it is unable to reverse LTD after it is established (DHPG+AM).

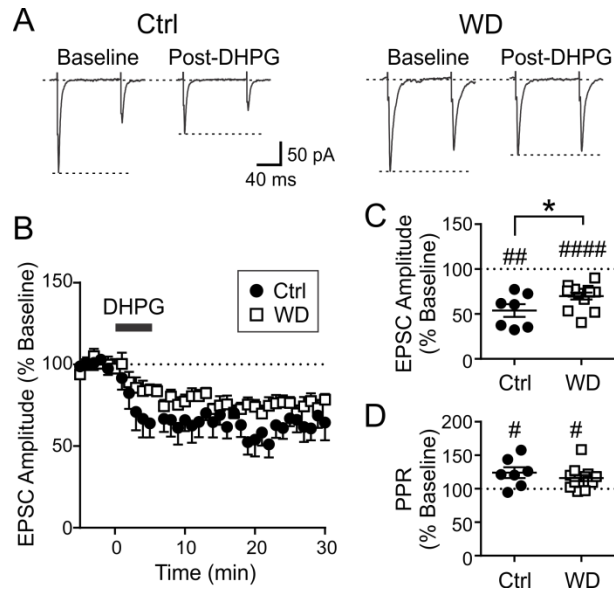$*p<0.05$, $**p<0.01$, for comparisons of different experimental groups

Figure 5: Group 1 mGluR activation induces presynaptic LTD regardless of diet.

A) Sample EPSCs recorded from Ctrl or WD orexin neuron during baseline or 25-30 minutes after DHPG (50μM) application.

B) Time-effect plot of EPSC amplitude with application of DHPG.

C and D) EPSC amplitude (C) and PPR (D) following DHPG application. DHPG induces LTD in both Ctrl and WD conditions, however the magnitude of LTD is greater in Ctrl.

*p<0.05 Ctrl vs WD; #p<0.05, ##p<0.01, ####p<0.0001 baseline vs post-DHPG
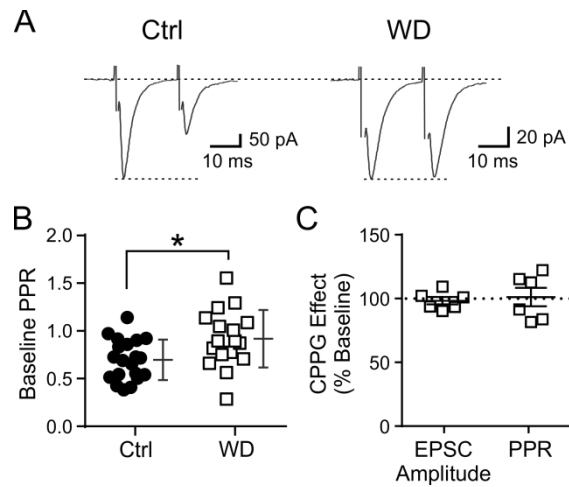
Figure 6: WD induces presynaptic inhibition independent of group III mGluR.

- A) Sample traces of paired EPSCs recorded from orexin neurons in Ctrl and WD conditions.
- B) WD increases baseline PPR in orexin neurons.
- C) Group III mGluR antagonist CPPG (200μM) has no effect on EPSC amplitude or PPR in WD orexin neurons.
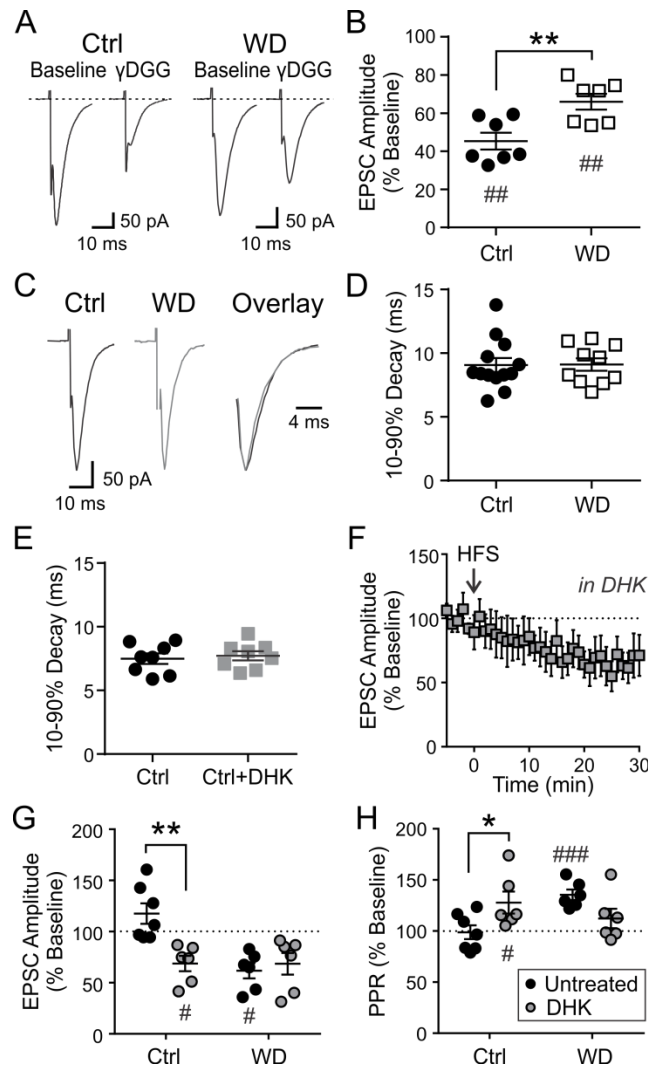
*p<0.05

Figure 7: Reduced synaptic glutamate clearance may underlie the unmasking of LTD by WD.

A) Sample EPSCs showing the effect of the low-affinity, competitive AMPA receptor antagonist γDGG (1mM) on EPSC amplitude in orexin neurons.

B) EPSC amplitude is less sensitive to the inhibitory effect of γDGG in WD than in Ctrl.

C) Sample EPSCs (without drug or HFS treatment) and their overlay showing similar decay times in Ctrl and WD conditions.

D) Diet has no effect on the 10-90% decay time of AMPA receptor-dependent EPSCs.

E) GLT-1 inhibitor DHK (10-15μM) has no effect on the 10-90% decay time of AMPA receptor-dependent EPSCs.

F) Time-effect plot showing that HFS induces LTD in the presence of DHK in the chow Ctrl condition.

G and H) Normalized ESPC amplitude (G) and PPR (H) post-HFS in Ctrl or WD orexin cells. HFS was applied in the absence (untreated; black circle) or presence of DHK (gray circle). LTD is primed by DHK in Ctrl but not WD condition.

*p<0.05, **p<0.01 comparing between experimental groups; #p<0.05, ### p<0.001 baseline vs post-HFS; ##p<0.005 baseline vs. γDGG.
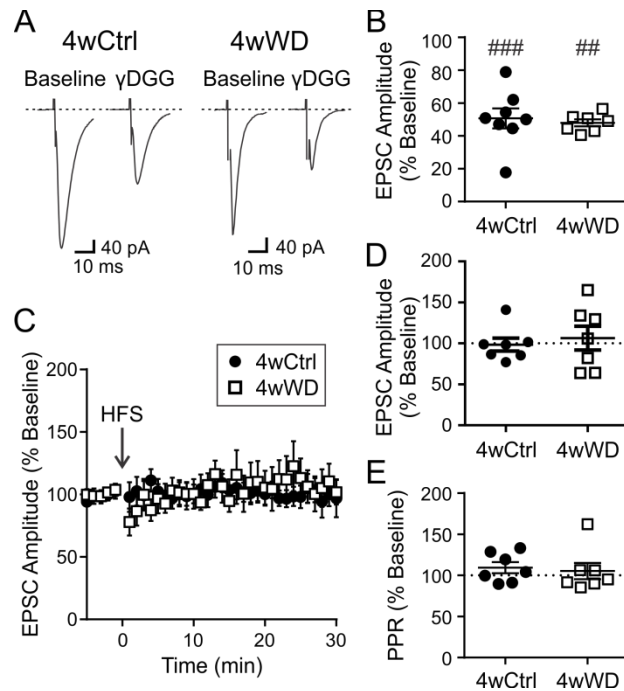
Figure 8: Prolonged WD feeding reverses synaptic priming for LTD in orexin neurons.

A) Sample EPSCs before and during γDGG (1mM) application in orexin neurons from rats fed WD for 4 weeks (4wWD) and age-matched controls (4wCtrl).

B) Inhibitory effect of γDGG on EPSC amplitude is not different between 4wWD and 4wCtrl.

C) Time-effect plot of HFS on EPSC amplitude showing a lack of HFS effect in orexin neurons from 4wCtrl or 4wWD groups.

D and E) EPSC amplitude (D) and PPR (E) are not affected by HFS after 4 weeks of control chow or WD.

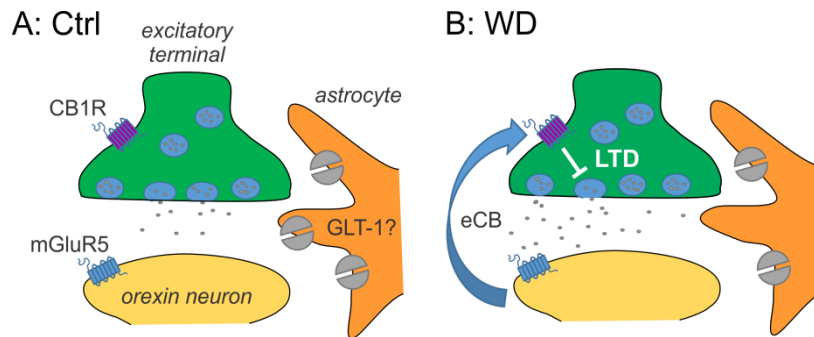##$p<0.01$, ### $p<0.001$ baseline vs. γDGG.

Figure 9: Proposed mechanism of LTD in orexin neurons.

A) In chow-fed condition (Ctrl), synaptically released glutamate is efficiently removed by transporters such as GLT-1, preventing perisynaptic mGluR5 activation.
B) In WD-fed condition, synaptic glutamate is not efficiently cleared and spills over during high intensity synaptic activity. This activates mGluR5 and subsequent retrograde endocannabinoid (eCB) signaling to CB1R-expressing excitatory synaptic terminals, resulting in presynaptic LTD.